Published in final edited form as:
Neurobiol Aging. 2012 January ; 33(1): 9–20. doi:10.1016/j.neurobiolaging.2010.01.014.

Fractional anisotropy of water diffusion in cerebral white matter across the lifespan

P. Kochunov[1,2], **D.E. Williamson**[1,3,4], **J. Lancaster**[1], **P. Fox**[1], **J Cornell**[4], **J. Blangero**[2], and **DC Glahn**[1,5]

[1]Research Imaging Institute, University of Texas Health Science Center at San Antonio.

[2]Southwest Foundation for Biomedical Research. San Antonio, Texas

[3]Department of Psychiatry, University of Texas Health Science Center at San Antonio, Texas

[4]Department of Epidemiology & Biostatistics, University of Texas Health Science Center at San Antonio, Texas

[5]Department of Psychiatry, Yale University & Olin Neuropsychiatric Research Center, Connecticut.

Abstract

Determining the time of peak of cerebral maturation is vital for our understanding of when cerebral maturation ceases and the cerebral degeneration in healthy aging begins. We carefully mapped changes in fractional anisotropy (FA) of water diffusion for eleven major cerebral white matter tracts in a large group (831) of healthy human subjects aged 11–90. FA is a neuroimaging index of micro-structural white matter integrity, sensitive to age-related changes in cerebral myelin levels, measured using diffusion tensor imaging. The average FA values of cerebral white matter (WM) reached peak at the age 32±6 years. FA measurements for all but one major cortical white matter tract (cortico-spinal) reached peaks between 23 and 39 years of age. The maturation rates, prior to age-of-peak were significantly correlated (r=0.74; p=.01) with the rates of decline, past age-of-peak. Regional analysis of corpus callosum (CC) showed that thinly-myelinated, densely packed fibers in the genu, that connect pre-frontal areas, maturated later and showed higher decline in aging than the more thickly myelinated motor and sensory areas in the body and splenium of CC. Our findings can be summarized as: associative, cerebral WM tracts that reach their peak FA values later in life also show progressively higher age-related decline than earlier maturing motor and sensory tracts. These findings carry multiple and diverse implications for both theoretical studies of the neurobiology of maturation and aging and for the clinical studies of neuropsychiatric disorders.

*For correspondence and reprint information contact: Peter Kochunov, Ph.D, Dip ABMP., University of Texas Health Science Center at San Antonio, Research Imaging Center, 7703 Floyd Curl Drive, San Antonio, Texas 78284, kochunov@uthscsa.edu, 210-567-8100 phone, 210-567-8152 Fax.

Disclosure Statement
The authors have no relevant information to disclose.

Introduction

Prevailing trends in cognitive development and normal aging suggest that there is an age when cognitive performance will reach a peak indicating the end of cerebral maturation and the beginning of cerebral decline(Salthouse, 2009). There is little doubt that cognitive changes in early maturation are associated with changes in brain integrity and there is growing evidence that a similar relationship underwrites the decline in cerebral integrity and cognitive functioning later in life (Bartzokis, 2004,Bartzokis, et al., 1999,Bartzokis, et al., 2008,Bastos Leite, et al., 2004,P. Kochunov, et al., 2009a,P. Kochunov, et al., 2009,Prins, et al., 2004,Schiavone, et al., 2009). However, it is not exactly known when cerebral maturation ceases and the degeneration associated with healthy aging begins. Determining the zenith of development is vital for both practical and theoretical reasons. From a practical perspective, it is important to know the age of onset of cerebral decline as this would represent an optimal time for intervention to slow or ideally prevent this decline. From a theoretical perspective, this knowledge is vital for the development of realistic neurobiological models of normal development and aging and specifically to understanding of neurodegenerative processes and genetic factors that predispose one to deviation from normal aging. A recent study of cognitive functioning in 2350 participants reported improvements in reasoning, spatial visualization and speed of processing into the 3rd and 4th decades of life, after which point cognitive processing showed a rapid age-related decline (Salthouse, 2009). To the extent that cognitive ability indexes brain maturation, these data suggest that development continues well into middle age. Although the neurobiological processes associated with the observed cognitive trends are unknown, Fleschsig proposed that continued myelination of white matter (WM) tracts could be a basis for later life brain development and subsequent improved cognitive efficiency (Flechsig, 1901). Herein we tested Fleschig's theory by assessing white matter (WM) integrity across the lifespan to determine how and when these measures peak in a large cohort of healthy individuals. Toward that end, we use diffusion tensor imaging (DTI) methods to provide an in vivo measure of changes in white matter myelin integrity indexed by fractional anisotropy (FA) of water diffusion.

DTI assessed FA describes the directional selectivity of the random diffusion of water molecules (Basser, 1994,Conturo, et al., 1996,Pierpaoli and Basser, 1996,Ulug, et al., 1995). Higher FA values (maximum theoretical value is 1.0) are observed along heavily myelinated WM tracts. The structure of the axonal cell membranes and myelin sheath hinders the diffusion of water molecules in all but the direction along the fiber tract, therefore producing highly anisotropic water diffusion (Pierpaoli and Basser, 1996). In contrast, a tissue where the water molecule motion is random and isotropic, such CSF, have FA values that are close to zero. Absolute WM FA values are sensitive to many parameters including regional myelination levels, the degree of intra-voxel fiber crossing, axonal density and average axonal diameter (Beaulieu, 2002). However, changes in regional FA values during normal maturation, aging and disorders are thought to be predominantly due to changes in myelination and can therefore be used as indirect measurement of myelin level (Budde, et al., 2007,Madler, et al., 2008,Song, et al., 2003,Song, et al., 2005).

Consistent with Fleschsig's regional findings, neonatal WM FA values in associative brain areas are much lower (by about 50%) than in the primary motor and sensory tracts (Ben Bashat, et al., 2005,Gao, et al., 2009,Hermoye, et al., 2006). Additionally, regional developmental trends in FA replicate the spatial-temporal course described by Fleschsig (Gao, et al., 2009). A recent longitudinal study of normal development showed that FA of the unimodal areas increased rapidly in the first and seconds years of life but showed little change in the next year (Gao, et al., 2009). FA of the multimodal areas continued to rise until mid adulthood (Ben Bashat, et al., 2005,Gao, et al., 2009) During normal aging, WM

FA declines with age and the regional trends of this decline parallel those described by Flechsig, with multimodal, associative WM areas showing higher decline rates than unimodal, sensory and motor areas (Abe, et al., 2002,Abe, et al., 2008,Hsu, et al., 2009,Kochunov, et al., 2007,Lehmbeck, et al., 2006,Moseley, 2002,Salat, et al., 2005,Sullivan and Pfefferbaum, 2003). In, our previous studies of aging trends in FA we showed that late-developing, multimodal associative fibers had a disproportionately higher sensitivity to aging than earlier-developing unimodal motor and sensory fibers (P. Kochunov, et al., 2009,Kochunov, et al., 2007). The biological mechanisms of FA changes with age are yet unknown. The rise in FA during development is associated with decline in radial diffusivity and therefore is thought to be due to myelination (Ben Bashat, et al., 2005,Gao, et al., 2009). The decline in FA with age was shown to be associated with reduction in density of glial cells and an apparent reduction in myelin levels (P. Kochunov, et al., 2009a,Madler, et al., 2008,Peters, et al., 2000).

Importantly, recent evidences suggest that life-long changes in the integrity of associative WM are linked with changes in cognition (Bartzokis, 2004,Bartzokis, et al., 2003,Bartzokis, et al., 2008,Charlton, et al., 2009,Kennedy and Raz, 2009,P. Kochunov, et al., 2009a,P. Kochunov, et al., 2009,Schiavone, et al., 2009,Vernooij, et al., 2009). Specifically, FA values in associative WM areas were correlated with the performance on the neuropsychological tests sensitive to processing speed, the speed with which information is mentally processed (Bartzokis, et al., 2008,Konrad, et al., 2009,Muetzel, et al., 2008). Additionally, our group and others have shown that higher frontal lobe FA values were associated with better performance on neuropsychological tests of executive function (P. Kochunov, et al., 2009,Konrad, et al., 2009). Similar trends were observed in normal aging where the intersubject variability in the integrity of the associative WM measured using DTI-FA and T2-relaxation-based myelin level mapping methods was found to be predictive of decline in processing speed (Bartzokis, et al., 2008,P. Kochunov, et al., 2009a,Schiavone, et al., 2009). Our recent work showed that in normal aging, over 50% of the intersubject variability in PS was explained by the decline in cerebral WM integrity measurements, with FA of thinly myelinated frontal WM tracts having the highest (~35%) explanatory power(P. Kochunov, et al., 2009a). This and other findings indicated that changes in basic neurocognitive functions such as processing speed and executive function across the lifespan were related to changes in the integrity of thinly myelinated, associative WM areas of the brain. The biological mechanism of this relationship appears to be due to changes in the propagation speed of action potentials across cortical networks (Ashe and Georgopoulos, 1994,Bartzokis, et al., 2008,Lutz, et al., 2005).

Recent studies showed that across the lifespan, FA of cerebral WM follows a quadratic trajectory, which peaks in early-to-middle adulthood (Hasan, et al., 2009a,Hasan, et al., 2009b,McLaughlin, et al., 2007). However, these studies were limited to just two brain regions, corpus callosum (CC) and uncinate fasciculus and methodological limitations, such as a small number of subjects, resulted in high uncertainty in the calculations of ages at which FA peaked (20.0±23.5 and 30.5± 16.0 years for CC and uncinate fasciculus, respectively)(Hasan, et al., 2009a,Hasan, et al., 2009b). In this work, we attempt to clarify regional age-related FA trends in a large population of subjects covering eight decades of human life-span. We used Fleschsig's report as the *a priori* hypothesis and set out to measure the age of peak of FA in eleven major WM tracts. To perform the by-tract analysis of WM integrity, we used a recently developed analytic method, tract-based spatial statistics (TBSS) (Smith, et al., 2006a,Smith, et al., 2007). TBSS was developed to overcome the limitations of voxel-based analysis of DTI data. Spatial resolution of DTI studies is generally inadequate for intersubject voxel-based analysis producing misalignment and partial-volume averaging effects(Smith, et al., 2006b). However, TBSS method addresses this by extracting the spatial course of major WM tracts and then analyzing FA values that

correspond to the middle of the tract. Previously, we used TBSS analysis to show that FA of associative WM tracts was sensitive to age-related changes in cortical GM thickness, sulcal and gyral spans, the volume of hyper-intense WM lesions (P. Kochunov, et al., 2009b,Kochunov, et al., 2007) as well as changes in executive function (P. Kochunov, et al., 2009) and processing speed(P. Kochunov, et al., 2009a).

Materials and Methods

Subjects

Analyses were performed on data from 831 (346 males/485 females) subjects recruited from suburban San Antonio, Texas. Subject's age ranged from 11–90, average age = 36.4±21.1 years (Table 1) however the age distribution was skewed with 254 subjects between ages 11 and 15. Additionally, 503 subjects (average age = 44.1±17.3 years) were from 79 families with the average family size = 6.4±7.9 subjects per family, ranging from 2 to 37 individuals. Subjects were excluded for MRI contraindications, history of neurological illnesses, stroke or other major neurological event. All experiments were performed with IRB approval and all subjects signed an informed consent. For minors, children and their parents signed assents and informed consents, respectively.

Diffusion tensor imaging

Diffusion tensor imaging was performed at the Research Imaging Institute, University of Texas Health Science Center at San Antonio, on a Siemens 3T Trio scanner using an eight-channel head coil. A single-shot, echo-planar, single refocusing spin-echo, T2-weighted sequence was used to acquire diffusion-weighted data with a spatial resolution of 1.7×1.7×3.0mm. The sequence parameters were: TE/TR=87/8000ms, FOV=200mm, axial slice orientation with 50 slices and no gaps, 55 isotropically distributed diffusion weighted directions, two diffusion weighing values b=0 and 700 s/mm2 and three b=0 images. The image acquisition time was 8 minutes. The number of diffusion directions, number of b=0 images and the magnitude of the b values were calculated using an optimization technique that maximizes the contrast to noise ratio based on the average diffusivity of the cerebral WM and the T2 relaxation times (Jones, et al., 1999).

TBSS processing

A tract-based spatial statistics (TBSS) method, distributed as a part of FMRIB Software Library (FSL) package, was used for tract-based analysis of diffusion anisotropy (Smith, et al., 2006a). First, fractional anisotropy (FA) images were created by fitting the diffusion tensor to the raw diffusion data (Smith SM, 2002). In the next step, all FA images were globally spatially normalized and then nonlinearly aligned to a group-wise, minimal-deformation target (MDT) brain. The global spatial normalized was performed using a method distributed with FSL package (FLIRT) (Smith, et al., 2006a) with 12 degrees of freedom. This step was performed to reduce the global intersubject variability in brain volumes prior to non-linear alignment. The group's MDT brain is identified by warping all individual brain images in the group to each (Kochunov, et al., 2001). The MDT is selected as the image that minimizes the amount of the required deformation from other images in the group. Next, individual FA images are averaged to produce a group-average anisotropy image. This image is used to create a group-wise skeleton of WM tracts. The skeletonization procedure is a morphological operation, which extracts the medial axis of an object. This procedure is used to encode the medial trajectory of the WM fiber-tracts with one-voxel thin sheaths.

Finally, FA values from each image are projected onto the group-wise skeleton of WM structures. This step accounts for residual misalignment among individual WM tracts. FA

values are assigned to each point along a skeleton using the peak value found within a designated range perpendicular to the skeleton. The FA values vary rapidly perpendicular to the tract direction but very slowly along the tract direction. By assigning the peak value to the skeleton, this procedure effectively maps the center of individual WM tracts on the skeleton. This processing is performed under two constraints. A distance map is used to establish search borders for individual tracts. The borders are created by equally dividing the distance between two nearby tracts. Secondly, a multiplicative 20mm full width at half-max Gaussian weighting is applied during the search to limit maximum projection distance from the skeleton.

Tract-based analysis

The population-based, 3D, DTI cerebral WM tract atlas developed in John Hopkins University (JHU) and distributed with the FSL package (Wakana, et al., 2004) was used to calculate population average diffusion parameter values along the spatial course of nine, major WM tracts (Table 1, Figure 1). The JHU atlas was non-linearly aligned to the MDT brain and image containing labels for individual tracts was transferred to MDT space using nearest-neighbor interpolation. Per-tract average values were calculated by averaging the values along the tracts in both hemispheres. The overall average FA values were calculated by averaging values for the entire WM skeleton.

Statistical analysis

We employed the statistical approach previously used by Hasan and colleagues in their studies of mapping of FA values across the lifespan (Hasan, Iftikhar et al. 2009; Hasan, Kamali et al. 2009). This analysis consists of two steps. First, the age of peak is calculated by fitting the entire dataset with a second order polynomial function. In addition, we expanded our model to include effects of sex, and sex*age and sex*age^2 interactions. In the second step, linear rates of maturation and decline are calculated by piece-wise fitting of the data from the subjects on the opposite sides from the age-of-peak using a linear function that also includes effects of sex, and sex*age interactions. A large number of our subjects (503) subjects had relatives who also participated in this study, the effects familial aggregations were modeled using a general linear mixed effect (GLME) model. A GLME model is capable of partitioning the intersubject variance into fixed (age, sex and their interactions) and mixed (within-family) effects. Modeling familial aggregations using GLME model allows making the results of the study more representative for a sample of independent subjects.

Estimation of peak age—FA values were modeled as a quadratic function of age and gender using the general linear mixed effect model presented in equation 1.

$$FA_{i,j} \sim \mathrm{A} + \beta_{age} Age_{i,j} + \beta_{age^2} Age_{i,j}^{\,2} + \beta_{sex} Sex_{i,j} + \beta_{age,sex} Age_{i,j} \cdot Sex_{i,j} + \beta_{age^2,sex} Age_{i,j}^{\,2} \cdot Sex_{i,j} + \alpha_{i,j} \quad (1)$$

Where $FA_{i,j}$ is the fractional anisotropy for the "j^{th}" subject from the "i^{th}" family, A is the constant FA term, βs are the covariate regression coefficients and $\alpha_{i,j}$ is a coefficient that accounts for random effects. This modeling was performed with the [R] package(R-Development-Core-Team, 2009) using the linear mixed effects model library and the maximum likelihood estimation algorithm (Pinheiro, et al., 2008). The subjects sex was coded as (0:1; F:M). The results of the modeling are the standardized regression coefficients (β) for and the standard errors that estimate linear associations between criterion variables

(FA) and fixed and interaction effects of age and sex. The level of statistical significance was set at $p \leq .001$ to reduce the probability of Type 1 errors associated with multiple (12) comparisons. Age-of-peak for the average and by-tract FA measurements, that did not show significant gender or gender by age interactions, was calculated as follows:

$$Age - of - peak = -\frac{\beta_{age}}{2 \cdot \beta_{age^2}} \quad (2)$$

The age-of-peak for FA measurements that showed significant gender effects was calculated as the average age-of-peak for males and females.

FA maturation and decline rates—Age-related maturation and decline rates were estimated by fitting FA measurements before and after age-of-peak using a simpler linear mixed effects model as follows:

$$FA_{i,j} \sim A + \beta_{age} Age_{i,j} + \beta_{sex} Sex_{i,j} + \beta_{age,sex} Age_{i,j} \cdot Sex_{i,j} + \alpha_{i,j} \quad (3)$$

Results

Significance of fixed effects (age and gender)

Beta coefficients and their significance for age and gender effects for the average and by-tract FA values are shown in Tables 3A. Additional analysis was done by segmenting the corpus callosum (CC) into three equal partitions along the A-P direction: genu, body and splenium (Table 2B). The second-order polynomial age-and-gender effects explained about 24% ($r=0.49$, $p<1E-16$) of the intersubject variability in the average FA values (Table 3A). Regionally, the quadratic model was significant ($p \leq .001$) for eight out of nine tracts and all three partitions of CC. The highest significance was observed for CR, where the quadratic model explained up to 34% of intersubject variability ($r=.58$, $p<1E-16$) (Figure 3). The quadratic model was not significant ($r=.17$, $p=0.003$) for the FA of cortico-spinal Tract (Figure 3). Significant ($p \leq 0.001$) age^2*sex interactions were observed for the average FA, cingulum, cortico-spinal tract and splenium of CC. A significant age*sex interaction was observed for the Splenium. The sign of the gender effect and interaction coefficients indicated that the males had slightly higher average FA values and slightly higher rates of FA decline with age.

The age-of-peak was calculated for eight of nine tracts and all three partitions of CC. The age-of-peak for the average FA was 32.1±5.9 years (Table 2A). The age-of-peak varied by WM tract, ranging from 23.1±11.6 years for the Sagittal Stratum to 39.4±5.6 for the cingulum (Tables 2A,B). The age of peak was not significantly correlated with the average FA value per tract ($r=.24$; $p=.5$).

Age-related maturation trends were significant ($p \leq .001$) for the average FA values, for three cerebral tracts and for all three partitions of the CC ($p \leq 0.001$), Tables 3 A,B. The largest age-related increases were observed for the CC and specifically for its middle third, CC body, where the FA increased with age at the annual rate of 0.002 (Table 3B). Age-related decline trends were significant for eight of nine tracts and for all three partitions of the CC. The largest declines with age were also observed in the CC and specifically in its anterior portion, the genu, where FA values declined at the annual rate of ~0.003 (Table 3B).

The age-related maturation and decline rates calculated using equation 3 were significantly correlated with each other ($r=0.74$; $p=.01$). Maturation and decline rates were not

significantly correlated with the average FA values (r=.35 and .42; p=.3 and .2, respectively). Though maturation rates were not significantly correlated with the age-of-peak (r=.35; p=.3), correlation was closer to significance for age-related rates past age-of-peak (r=0.60; p<.1) (Figure 4 and Figure 5). The correlation between age-of-peak and average FA values per tract was also not significant (r=.24; p=.7).

Significance of mixed effects (familial aggregation)

Significance of the within-group dependence due to familial aggregations was tested using two statistical approaches provided by [R] statistical analysis software(R-Development-Core-Team, 2009). First, we calculated the logarithm of the ratio of the likelihoods for two models: one that accounted for familial aggregations and one that did not, as suggested in (Pinheiro and Bates, 2000). Additionally, significance of within-group dependence was tested by modeling mixed-effects parameters using a Markov-Chain Monte-Carlo method (Baayen, et al., 2008,Bates, 2009). Both methods reported that familial aggregation was statistically significant: p=0.005 for log likelihood ratios and p=0.01 for Monte-Carlo modeling.

Discussion

This is the first comprehensive report, to our knowledge, where the temporal trajectories of fractional anisotropy (FA) of major WM tracts has have been carefully mapped in a large group of healthy subjects covering over 8 decades of human life span. Previous work by Hassan and colleagues suggested that FA for uncinate fasciculus and CC reaches the peak in the adulthood (age-of-peak=20.0±23.5 and 30.5± 16.0 years, respectively) but their estimates had a moderate degree of uncertainty due to a small number of subjects (Hasan, et al., 2009a,Hasan, et al., 2009b). This study demonstrated with a high degree of certainty that cerebral integrity for all but one WM tract increased with age during childhood and early adulthood, reaching full maturity during the 3rd and 4th decades of life (23.1–39.4 years) and declined with age thereafter. One exception was the corticospinal tract (CST), which showed no significant age related trends (Figure 3). The CST is unique among the cortical WM bundles as it is known to be partially myelinated at birth(Flechsig, 1901). A recent longitudinal DTI study performed in healthy infants showed that average CST's FA values in the newborns were significantly higher than the average FA values in the peripheral frontal WM. The average FA values for CST reach maturity during the first two years of life and remained relatively unchanged after that (Gao, et al., 2009). Additionally, we used the methodology proposed by Hassan et al. (Hasan, et al., 2009a,Hasan, et al., 2009b) to estimate the linear rates of maturation and decline that preceded and followed the age-of-peak. As predicted, the rate at which FA increased during maturation was significantly correlated with the rate of decline (r=0.74; p=.01) (Figure 4). The rate of maturation was not significantly correlated with the tract's average FA value or with the age-of-peak of FA values. However, the correlation between the age of peak and the rate of decline approached statistical significance (r=0.60; p<.1, n=9)

The biological basis of regional changes in WM FA during lifespan is not fully understood but changes in axonal myelination are considered as likely cause (Abe, et al., 2002,Gao, et al., 2009). Methodologically, the absolute FA values are only indirect indicators of regional myelination levels as absolute FA values are also sensitive to the intra-voxel changes in fiber orientation (Budde, et al., 2007,Song, et al., 2003,Song, et al., 2005). For example, the corpus callosum (CC) is composed of the fiber bundles that originate in the corona radiata. However, its average FA value (FA=0.66±0.04) is substantially higher than the average FA of corona radiata (FA=0.46±0.02). This difference in the average FA values is primarily due to differences in spatial complexity between them. The fiber bundles located in the corona radiata follow a geometrically complex path, with a high degree of intra-voxel changes in

fiber orientation, before reaching CC (Hasan, et al., 2009b,Wakana, et al., 2004). Once within CC, these fibers become predominantly oriented in the L-R direction and their higher spatial coherence is responsible for much higher average FA (Hasan, et al., 2009b,Wakana, et al., 2004). In contrast, intersubject variance in regional FA have been reported to be predominantly (70–80%) due to the differences in regional myelination levels (Madler, et al., 2008). Furthermore, longitudinal studies in humans and studies in animal models, where levels of myelination were carefully manipulated, showed that changes in WM FA were primarily driven by changes in the radial diffusivity e.g. diffusivity across the axonal membranes (Budde, et al., 2007,Gao, et al., 2009,Song, et al., 2003,Song, et al., 2005). Radial diffusivity is a measurement of a restricted diffusivity across the axonal walls. Biologically, this measurement relates the permeability of axonal membranes and therefore serves as an indirect estimate of axonal myelination level. Consistent with these findings, intersubject variability in the average FA in this sample showed a higher correlation with radial diffusivity ($r=0.75$, $p<1E-24$) than with longitudinal diffusivity ($r=0.45$, $p<1E-24$) e.g. diffusivity along the axonal direction.

Regional FA trends were consistent with Fleschsig findings regarding intermediate and later-term changes in cerebral myelination levels. In his classic 1901 manuscript, Fleschsig, reported that myelination of the human cerebrum continues well into late adulthood(Flechsig, 1901). He identified that the earliest cerebral areas to begin myelination, the primordial zones, are the areas responsible for primary motor and sensory functions, such as the cortico-spinal tract. The intermediary zones, the cortical areas responsible for higher level of processing of motor and sensory information, such as pre-motor and parietal cortexes, myelinated in late childhood. The areas that continued to myelinate into the early adulthood, the terminal zones e.g. superior frontal and cingulate cortexes, are the areas known to be responsible for higher order, multimodal cognitive function. The WM tracts that carry higher level sensory and motor information: sagittal striatum, and external capsule reach peak FA in the 3rd decade of life. The WM tracts that connect multimodal areas of the brain, e.g. cingulum, CC and fronto-occipital tracts reach peak FA later in the 4th decade of life (Tables 2A,B). Fleschsig's findings regarding earlier myelinated trends were confirmed by a recent study that measured DTI FA measurements in healthy infants (Gao, et al., 2009). By the age of 3 years, the average FA value for the cortico-spinal tract were approaching adult levels (~0.6) and about twice the average FA value in the peripheral frontal WM indicating that maturation of CST is completed in early childhood.

The biological basis of regional heterochronicity of cerebral myelination is not fully understood. Microscopy studies clearly determined that oligodendrocytes that myelinate primary motor and sensory tracts are morphologically distinct from the glial cells that myelinate the associative tracts connecting multimodal areas (Pfefferbaum, et al., 2000,Sullivan, et al., 2001,Wood P. and Bunger RP., 1984). The primary motor and sensory WM tracts, mainly composed of large diameter axons, are being myelinated by a single oligodendrocyte per myelin segment (Wood P. and Bunger RP., 1984). In contrast, a single oligodendrocyte in associative WM ensheathes up to 50 axons (Lamantia and Rakic, 1990,Wood P. and Bunger RP., 1984). The latter type of oligodendrocytes produce far fewer myelin layers per axon (less myelin) than the glia located in the primary sensory and motor tracts(Lamantia and Rakic, 1990). Additionally, the oligodendrocytes of the associative WM tracts have reduced rates of myelin turn over and slower rates of myelin repair (Hof, et al., 1990,Wakana, et al., 2004). To evaluate the heterogeneity between two types of WM fibers, we analyzed age-related FA trends in three partitions of the CC. Unlike most other cerebral WM tracts, which carry a mixture of heavily and thinly myelinated fibers, the fiber tracts that compose the CC fiber are spatially distributed along its anterior-posterior axis.

The corpus callosum (CC) is the largest commissural projection system in the CNS. Studies in non-human primates and humans have shown that the CC is composed of distinct fiber types that can be roughly segmented along its A-P dimension into three regions: genu, body and splenium each occupying ~1/3 of the A-P CC length (Aboitiz, 1992,Aboitiz, et al., 1992,Kochunov, et al., 2005a,Lamantia and Rakic, 1990,Witelson, 1989). The genu (anterior third of the CC) mainly contains the thinly myelinated and unmyelinated, smaller diameter, densely packaged associative fibers that connect the bilateral prefrontal cortices; the body (middle third) primarily contains more thickly myelinated commissural fibers for motor, somatosensory and auditory cortices and the splenium (posterior third) carries thickly myelinated commissural fibers, intermixed with small number of thinly myelinated fibers, connecting the temporal, parietal and occipital lobes (Aboitiz, 1992,Aboitiz, et al., 1992,Kochunov, et al., 2005a,Lamantia and Rakic, 1990,Witelson, 1989). Previously, we demonstrated that the volume of heavily myelinated posterior portions of CC, the body and the splenium, were markedly smaller in individuals with a genetic, disorder (18q−) characterized by haploinsufficiency of the myelin basic protein (MBP) when compared to the healthy controls(Kochunov, et al., 2005a). In contrast, the thinly myelinated genu of CC did not show a significant difference between two groups (Kochunov, et al., 2005a). In the present study, we observed that the posterior segments of CC, body and splenium reach the age-of-peak progressively sooner and showed lower rates of age-related decline than the thinly myelinated, associative fibers in the genu (Table 3B). This finding replicated previous reports from our group and others, which showed that age-related decline in the FA values for the genu of CC was the steepest among the WM tracts (Kochunov, et al., 2007,Pfefferbaum, et al., 2000,Sullivan, et al., 2001). Our interpretation of this trend is based the hypothesis proposed by Bartzokis and colleagues (Bartzokis, et al., 2001,Bartzokis, et al., 2003,Bartzokis, et al., 2004). The hypothesis is that oligodendrocites that myelinate the densely packed WM tracts that connect multimodal cortical areas are among the most metabolically active cells in the adult CNS. This therefore makes these cells, especially vulnerable to accumulation of metabolic damage (Bartzokis, 2004,Kochunov, et al., 2007).

We observed small but statistically significant gender by age^2 interaction for the average FA values and significant gender and gender by age^{1,2} interactions for the splenium of the CC (Table 2, Table 3). The linear rates of cerebral maturation were higher for males than females but this difference was not significant at the $p \leq .001$ level (Table 3A). However, male subjects had a significantly higher rate of FA decline (Table 3A) and similar observations were made by Sullivan, et al.(Sullivan, et al., 2001). Additionally, similar gender differences in normal age-related trends were reported by studies of age-related trends in other brain compartments (Good CD, et al., 2001,Kochunov, et al., 2005b,Raz N, et al., 1997,Xu J, et al., 2000). The sources of these differences are not clear, but neuro-protective properties of estrogen and environmental interactions have been proposed (den Heijer, et al., 2003,Eberling, et al., 2004).

The range in the ages-of-peak for individual cerebral tracts (23.1–39.4 years) falls within the age range during which the performance on various cognitive measurements was reported to reach its peak (22–42 years*)(Salthouse, 2009). The overlap between the ages of peak for cerebral FA values and neurocognitive function during the 3rd and 4th decades suggest fundamental implications for research and clinical studies of maturation, aging and disorders. From the research perspective, this implicates age-related changes in cerebral WM as the neurobiological mechanism associated with cognitive maturation and decline. This finding also suggests that diffusion tensor imaging could be a sensitive neuroimaging

*Age range during which longitudinal neurocognitive scores were not statistically significant from their peak values

method to study regional WM maturation and senescence trends. From a clinical perspective, the finding that the cerebral development continues into early adulthood is supportive of the hypothesis of disruptions in normal cerebral development in disorders such as anxiety, psychological trauma, and post-traumatic stress disorders (De Bellis and Thomas, 2003). It is postulated that the neurohormonal response to a traumatic event could cause an early halt in development of cerebral myelination, with progressively lower myelin levels in children who experienced this earlier in life (De Bellis and Thomas, 2003). From a clinical perspective, it is also important to know that the age-related decline in the associative WM tracts begins in the early-to-mid rather than in late adulthood. This could serve as justification for the period of starting intervention therapies before substantial damages take place. Mapping of FA can also provide a diagnostic tool to localize potential trouble areas or targets and a neuroimaging-based means to assess treatment efficacy for the therapies designed to stop or even reverse age-related decline.

A large number of our subjects (503 out of 831) had relatives who also participated in this study. The effects of this familial aggregation were separated from the effects of age and gender using a general linear mixed effects model. This model reported that effects of familial aggregation were statistically significant, indicating that there was a significant within-group dependence of FA measurements. This finding was expected; our analysis of heritability performed in this population indicated that over 50% of the intersubject variability in the average FA was explained by genetic factors (Kochunov, et al., 2010). Another recent study of DTI data from 92 twins (23 MZ and 23 DZ pairs also showed that average FA values of the bilateral frontal (h2=0.55, left; h2=0.74, right), bilateral parietal (h2=0.85, left; h2=0.84, right), and left occipital (h2=0.76) were under genetic control (Chiang, et al., 2009).

Limitations

The measurements presented in this manuscript are cross-sectional. There are limitations to the conclusions that can be made about longitudinal processes, such as aging, from cross-sectional data as longitudinal studies often fail to confirm the age-related trends obtained from cross-sectional data (Royall, et al., 2005). Therefore, further research is needed to confirm the cross-sectional trends observed here using a longitudinal design.

Another limitation of this study is the skewness in the distribution of age in our subjects. A large group of subjects (254) were between ages of 11 and 15 years (Table 1). The effect of the oversampling of the younger subjects is that the estimates of linear maturation rates were made with a higher precession than the estimates of the linear age-related decline rates. However, the remainder of our subjects was distributed more uniformly across the ages (Table 1) and we therefore consider this a minor limitation.

Conclusion

We carefully mapped the heterogeneity and heterochronicity of fractional anisotropy (FA) of water diffusion in a large group of healthy subjects aged 11 to 90 years. We showed that the ages-of-peak for the fractional anisotropy (FA) of major WM tracts were in the 3rd and 4th decades of life (23.1–39.4 years). The exception was the cortico-spinal tract that is known to reach its adult myelination levels in childhood. As hypothesized, the age-range where by-tract FA values reach their maximum overlapped with the age range during which the performance on various cognitive measurements peaked (Salthouse, 2009). The by-tract rates of cerebral maturation were significantly correlated (r=0.74; p=.01) with the rates of age-related decline following the age-of-peak. Regional analysis of corpus callosum (CC) showed that thinly-myelinated, densely packed fibers in the genu that connect pre-frontal

areas maturated later and showed higher age related decline than more thickly myelinated motor and sensory areas in the body and the splenium of the CC. We believe that our findings could have multiple and diverse implication for both theoretical studies of the neurobiology of aging and for clinical studies of neuropsychiatric disorders.

Acknowledgments

This research was supported by National Institute of Biomedical Imaging and Bioengineering (K01 EB006395) grant to P.K., the National Institute on Alcohol Abuse and Alcoholism (R01AA016274) to D.E.W., the National Institute of Mental Health (RO1s MH078111, MH0708143 and MH083824) to J.B. and D.G.. Research support was also provided by the Human Brain Mapping Project, which is jointly funded by NIMH and NIDA (P20 MH/DA52176), by General Clinical Research Core (HSC19940074H)

Reference

Abe O, Aoki S, Hayashi N, Yamada H, Kunimatsu A, Mori H, Yoshikawa T, Okubo T, Ohtomo K. Normal aging in the central nervous system: quantitative MR diffusion-tensor analysis. Neurobiol Aging. 2002; 23(3):433–441. [PubMed: 11959406]

Abe O, Yamasue H, Aoki S, Suga M, Yamada H, Kasai K, Masutani Y, Kato N, Ohtomo K. Aging in the CNS: comparison of gray/white matter volume and diffusion tensor data. Neurobiol Aging. 2008; 29(1):102–116. doi:S0197-4580(06)00330-7 [pii] 10.1016/j.neurobiolaging.2006.09.003. [PubMed: 17023094]

Aboitiz F. Brain connections: interhemispheric fiber systems and anatomical brain asymmetries in humans. Biol Res. 1992; 25(2):51–61. [PubMed: 1365702]

Aboitiz F, Scheibel AB, Fisher RS, Zaidel E. Fiber composition of the human corpus callosum. Brain Res. 1992; 598(1–2):143–153. [PubMed: 1486477]

Ashe J, Georgopoulos AP. Movement parameters and neural activity in motor cortex and area 5. Cereb Cortex. 1994; 4(6):590–600. [PubMed: 7703686]

Baayen RH, Davidson DJMBD. Mixed-effects modeling with crossed random effects for subjects and items. Journal of Memory and Language. 2008; 59(4):390–412.

Bartzokis G. Age-related myelin breakdown: a developmental model of cognitive decline and Alzheimer's disease. Neurobiol Aging. 2004; 25(1):5–18. [PubMed: 14675724]

Bartzokis G, Beckson M, Lu PH, Nuechterlein KH, Edwards N, Mintz J. Age-related changes in frontal and temporal lobe volumes in men: a magnetic resonance imaging study. Arch Gen Psychiatry. 2001; 58(5):461–465. [PubMed: 11343525]

Bartzokis G, Cummings JL, Markham CH, Marmarelis PZ, Treciokas LJ, Tishler TA, Marder SR, Mintz J. MRI evaluation of brain iron in earlier- and later-onset Parkinson's disease and normal subjects. Magn Reson Imaging. 1999; 17(2):213–222. [PubMed: 10215476]

Bartzokis G, Cummings JL, Sultzer D, Henderson VW, Nuechterlein KH, Mintz J. White matter structural integrity in healthy aging adults and patients with Alzheimer disease: a magnetic resonance imaging study. Arch Neurol. 2003; 60(3):393–398. [PubMed: 12633151]

Bartzokis G, Lu PH, Tingus K, Mendez MF, Richard A, Peters DG, Oluwadara B, Barrall KA, Finn JP, Villablanca P, Thompson PM, Mintz J. Lifespan trajectory of myelin integrity and maximum motor speed. Neurobiol Aging. 2008

Bartzokis G, Sultzer D, Lu PH, Nuechterlein KH, Mintz J, Cummings J. Heterogeneous age-related breakdown of white matter structural integrity: Implications for cortical "disconnection" in aging and Alzheimer's disease. Neurobiol Aging. 2004; 25(7):843–851. [PubMed: 15212838]

Basser PJ. Focal magnetic stimulation of an axon. IEEE Transactions on Biomedical Engineering. 1994; 41(6):601–606. [PubMed: 7927380]

Bastos Leite AJ, Scheltens P, Barkhof F. Pathological aging of the brain: an overview. Top Magn Reson Imaging. 2004; 15(6):369–389. [PubMed: 16041289]

Bates D. Linear mixed model implementation in lme4. University of Wisconsin - Madison. 2009

Beaulieu C. The basis of anisotropic water diffusion in the nervous system - a technical review. NMR Biomed. 2002; 15(7–8):435–455. doi:10.1002/nbm.782. [PubMed: 12489094]

Ben Bashat D, Ben Sira L, Graif M, Pianka P, Hendler T, Cohen Y, Assaf Y. Normal white matter development from infancy to adulthood: comparing diffusion tensor and high b value diffusion weighted MR images. J Magn Reson Imaging. 2005; 21(5):503–511. doi:10.1002/jmri.20281. [PubMed: 15834918]

Budde MD, Kim JH, Liang HF, Schmidt RE, Russell JH, Cross AH, Song SK. Toward accurate diagnosis of white matter pathology using diffusion tensor imaging. Magn Reson Med. 2007; 57(4):688–695. doi:10.1002/mrm.21200. [PubMed: 17390365]

Charlton RA, Schiavone F, Barrick TR, Morris RG, Markus HS. Diffusion Tensor Imaging detects age-related white matter change over a two-year follow-up which is associated with working memory decline. J Neurol Neurosurg Psychiatry. 2009 doi:jnnp.2008.167288 [pii] 10.1136/jnnp.2008.167288.

Chiang MC, Barysheva M, Shattuck DW, Lee AD, Madsen SK, Avedissian C, Klunder AD, Toga AW, McMahon KL, de Zubicaray GI, Wright MJ, Srivastava A, Balov N, Thompson PM. Genetics of brain fiber architecture and intellectual performance. J Neurosci. 2009; 29(7):2212–2224. doi:29/7/2212 [pii] 10.1523/JNEUROSCI.4184-08.2009. [PubMed: 19228974]

Conturo TE, McKinstry RC, Akbudak E, Robinson BH. Encoding of anisotropic diffusion with tetrahedral gradients: a general mathematical diffusion formalism and experimental results. Magn Reson Med. 1996; 35(3):399–412. [PubMed: 8699953]

De Bellis MD, Thomas LA. Biologic findings of post-traumatic stress disorder and child maltreatment. Curr Psychiatry Rep. 2003; 5(2):108–117. [PubMed: 12685990]

den Heijer T, Geerlings MI, Hofman A, de Jong FH, Launer LJ, Pols HA, Breteler MM. Higher estrogen levels are not associated with larger hippocampi and better memory performance. Arch Neurol. 2003; 60(2):213–220. doi:noc20072 [pii]. [PubMed: 12580706]

Eberling JL, Wu C, Tong-Turnbeaugh R, Jagust WJ. Estrogen- and tamoxifen-associated effects on brain structure and function. Neuroimage. 2004; 21(1):364–371. doi:S1053811903005457 [pii]. [PubMed: 14741674]

Flechsig P. Developmental (myelogenetic) localisation of the cerebral cortex in the human. Lancet. 1901; 158:1027–1030.

Gao W, Lin W, Chen Y, Gerig G, Smith JK, Jewells V, Gilmore JH. Temporal and spatial development of axonal maturation and myelination of white matter in the developing brain. AJNR Am J Neuroradiol. 2009; 30(2):290–296. doi:ajnr.A1363 [pii] 10.3174/ajnr.A1363. [PubMed: 19001533]

Good CD, Johnsrude IS, Ashburner J, Henson RN, Friston KJ, Frackowiak RS. A voxel-based morphometric study of ageing in 465 normal adult human brains. Neuroimage. 2001; 14(1 Pt 1): 21–36. [PubMed: 11525331]

Hasan KM, Iftikhar A, Kamali A, Kramer LA, Ashtari M, Cirino PT, Papanicolaou AC, Fletcher JM, Ewing-Cobbs L. Development and aging of the healthy human brain uncinate fasciculus across the lifespan using diffusion tensor tractography. Brain Res. 2009a; 1276:67–76. doi:S0006-8993(09)00776-8 [pii] 10.1016/j.brainres.2009.04.025. [PubMed: 19393229]

Hasan KM, Kamali A, Iftikhar A, Kramer LA, Papanicolaou AC, Fletcher JM, Ewing-Cobbs Lf. Diffusion tensor tractography quantification of the human corpus callosum fiber pathways across the lifespan. Brain Res. 2009b; 1249:91–100. doi:S0006-8993(08)02516-X [pii] 10.1016/j.brainres.2008.10.026. [PubMed: 18996095]

Hermoye L, Saint-Martin C, Cosnard G, Lee SK, Kim J, Nassogne MC, Menten R, Clapuyt P, Donohue PK, Hua K, Wakana S, Jiang H, van Zijl PC, Mori S. Pediatric diffusion tensor imaging: normal database and observation of the white matter maturation in early childhood. Neuroimage. 2006; 29(2):493–504. doi:S1053-8119(05)00585-9 [pii] 10.1016/j.neuroimage.2005.08.017. [PubMed: 16194615]

Hof PR, Cox K, Morrison JH. Quantitative analysis of a vulnerable subset of pyramidal neurons in Alzheimer's disease: I. Superior frontal and inferior temporal cortex. J Comp Neurol. 1990; 301(1):44–54. doi:10.1002/cne.903010105. [PubMed: 2127598]

Hsu JL, Van Hecke W, Bai CH, Lee CH, Tsai YF, Chiu HC, Jaw FS, Hsu CY, Leu JG, Chen WH, Leemans A. Microstructural white matter changes in normal aging: A diffusion tensor imaging study with higher-order polynomial regression models. Neuroimage. 2009 doi:S1053-8119(09)00943-4 [pii] 10.1016/j.neuroimage.2009.08.031.

Jones DK, Horsfield MA, Simmons A. Optimal strategies for measuring diffusion in anisotropic systems by magnetic resonance imaging. Magn Reson Med. 1999; 42(3):515–525. doi:10.1002/(SICI)1522-2594(199909)42:3<515::AIDMRM14>3.0.CO;2-Q [pii]. [PubMed: 10467296]

Kennedy KM, Raz N. Aging white matter and cognition: differential effects of regional variations in diffusion properties on memory, executive functions, and speed. Neuropsychologia. 2009; 47(3):916–927. doi:S0028-3932(09)00007-4 [pii] 10.1016/j.neuropsychologia.2009.01.001. [PubMed: 19166865]

Kochunov P, Coyle T, Lancaster J, Hardies J, Kochunov V, Bartzokis G, Royall D, Stanley J, Schlosser A, Fox P. Processing speed is correlated with cerebral health markers in the frontal lobes as quantified by neuro-imaging. Neuroimage. 2009a In press (10.1016/j.neuroimage.2009.09.052). doi:10.1016/j.neuroimage.2009.09.052.

Kochunov P, Glahn D, Lancaster J, Wincker P, Smith S, Thompson P, Almasy L, Duggirala R, Fox P, Blangero J. Genetics of microstructure of cerebral white matter using diffusion tensor imaging. Neuroimage. 2010 In Press.

Kochunov P, Lancaster J, Hardies J, Thompson PM, Woods RP, Cody JD, Hale DE, Laird A, Fox PT. Mapping structural differences of the corpus callosum in individuals with 18q deletions using targetless regional spatial normalization. Hum Brain Mapp. 2005a; 24(4):325–331. [PubMed: 15704090]

Kochunov P, Lancaster JL, Thompson P, Woods R, Mazziotta J, Hardies J, Fox P. Regional spatial normalization: toward an optimal target. J Comput Assist Tomogr. 2001; 25(5):805–816. [PubMed: 11584245]

Kochunov P, Mangin JF, Coyle T, Lancaster J, Thompson P, Riviere D, Cointepas Y, Regis J, Schlosser A, Royall DR, Zilles K, Mazziotta J, Toga A, Fox PT. Age-related morphology trends of cortical sulci. Hum Brain Mapp. 2005b; 26(3):210–220. [PubMed: 16161162]

Kochunov P, Ramage AE, Lancaster JL, Robin DA, Narayana S, Coyle T, Royall DR, Fox P. Loss of cerebral white matter structural integrity tracks the gray matter metabolic decline in normal aging. Neuroimage. 2009b; 45(1):17–28. [PubMed: 19095067]

Kochunov P, Robin D, Royall D, Lancaster J, Kochunov V, Coyle T, Schlosser A, Fox P. Can structural MRI cerebral health markers track cognitive trends in executive control function during normal maturation and adulthood? Hum Brain Mapp. 2009; 30(8):2581–2594. [PubMed: 19067326]

Kochunov P, Thompson PM, Lancaster JL, Bartzokis G, Smith S, Coyle T, Royall DR, Laird A, Fox PT. Relationship between white matter fractional anisotropy and other indices of cerebral health in normal aging: tract-based spatial statistics study of aging. Neuroimage. 2007; 35(2):478–487. [PubMed: 17292629]

Konrad A, Vucurevic G, Musso F, Stoeter P, Winterer G. Correlation of Brain White Matter Diffusion Anisotropy and Mean Diffusivity with Reaction Time in an Oddball Task. Neuropsychobiology. 2009; 60(2):55–66. doi:000236445 [pii] 10.1159/000236445. [PubMed: 19752579]

Lamantia AS, Rakic P. Cytological and quantitative characteristics of four cerebral commissures in the rhesus monkey. J Comp Neurol. 1990; 291(4):520–537. doi:10.1002/cne.902910404. [PubMed: 2329189]

Lehmbeck JT, Brassen S, Weber-Fahr W, Braus DF. Combining voxel-based morphometry and diffusion tensor imaging to detect age-related brain changes. Neuroreport. 2006; 17(5):467–470. [PubMed: 16543808]

Lutz K, Koeneke S, Wustenberg T, Jancke L. Asymmetry of cortical activation during maximum and convenient tapping speed. Neurosci Lett. 2005; 373(1):61–66. [PubMed: 15555778]

Madler B, Drabycz SA, Kolind SH, Whittall KP, MacKay AL. Is diffusion anisotropy an accurate monitor of myelination? Correlation of multicomponent T2 relaxation and diffusion tensor anisotropy in human brain. Magn Reson Imaging. 2008; 26(7):874–888. doi:S0730-725X(08)00083-0 [pii] 10.1016/j.mri.2008.01.047. [PubMed: 18524521]

McLaughlin NC, Paul RH, Grieve SM, Williams LM, Laidlaw D, DiCarlo M, Clark CR, Whelihan W, Cohen RA, Whitford TJ, Gordon E. Diffusion tensor imaging of the corpus callosum: a cross-sectional study across the lifespan. Int J Dev Neurosci. 2007; 25(4):215–221. doi:S0736-5748(07)00043-3 [pii] 10.1016/j.ijdevneu.2007.03.008. [PubMed: 17524591]

Moseley M. Diffusion tensor imaging and aging - a review. NMR Biomed. 2002; 15(7–8):553–560. [PubMed: 12489101]

Muetzel RL, Collins PF, Mueller BAAMS, Lim KO, Luciana M. The development of corpus callosum microstructure and associations with bimanual task performance in healthy adolescents. Neuroimage. 2008; 39(4):1918–1925. doi:S1053-8119(07)00956-1 [pii] 10.1016/j.neuroimage.2007.10.018. [PubMed: 18060810]

Peters A, Moss MB, Sethares C. Effects of aging on myelinated nerve fibers in monkey primary visual cortex. J Comp Neurol. 2000; 419(3):364–376. [PubMed: 10723011]

Pfefferbaum A, Sullivan EV, Hedehus M, Lim KO, Adalsteinsson E, Moseley M. Age-related decline in brain white matter anisotropy measured with spatially corrected echo-planar diffusion tensor imaging. Magn Reson Med. 2000; 44(2):259–268. [PubMed: 10918325]

Pierpaoli C, Basser PJ. Toward a quantitative assessment of diffusion anisotropy. Magn Reson Med. 1996; 36(6):893–906. [PubMed: 8946355]

Pinheiro, J.; Bates, D. Mixed-Effects Models in S and S-PLUS'. New York: Springer; 2000.

Pinheiro J, Bates D, DebRoy S, Sarkar D. nlme: Linear and Nonlinear Mixed Effects Models. 2008

Prins ND, van Dijk EJ, den Heijer T, Vermeer SE, Koudstaal PJ, Oudkerk M, Hofman A, Breteler MM. Cerebral white matter lesions and the risk of dementia. Arch Neurol. 2004; 61(10):1531–1534. [PubMed: 15477506]

R-Development-Core-Team. R: A Language and Environment for Statistical Computing. 2009

Raz N, Gunning FM, Head D, Dupuis JH, McQuain J, Briggs SD, Loken WJ, Thornton AE, Acker JD. Selective aging of the human cerebral cortex observed in vivo: differential vulnerability of the prefrontal gray matter. Cereb Cortex. 1997; 7(3):268–282. [PubMed: 9143446]

Royall DR, Palmer R, Chiodo LK, Polk MJ. Normal rates of cognitive change in successful aging: the freedom house study. J Int Neuropsychol Soc. 2005; 11(7):899–909. [PubMed: 16519269]

Salat DH, Tuch DS, Greve DN, van der Kouwe AJ, Hevelone ND, Zaleta AK, Rosen BR, Fischl B, Corkin S, Rosas HD, Dale AM. Age-related alterations in white matter microstructure measured by diffusion tensor imaging. Neurobiol Aging. 2005; 26(8):1215–1227. doi:S0197-4580(04)00317-3 [pii] 10.1016/j.neurobiolaging.2004.09.017. [PubMed: 15917106]

Salthouse TA. When does age-related cognitive decline begin? Neurobiol Aging. 2009; 30(4):507–514. [PubMed: 19231028]

Schiavone F, Charlton RA, Barrick TR, Morris RG, Markus HS. Imaging age-related cognitive decline: A comparison of diffusion tensor and magnetization transfer MRI. J Magn Reson Imaging. 2009; 29(1):23–30. [PubMed: 19097099]

Smith SM. Fast robust automated brain extraction. Hum Brain Mapp. 2002; 17(3):143–155. [PubMed: 12391568]

Smith SM, Jenkinson M, Johansen-Berg H, Rueckert D, Nichols TE, Mackay CE, Watkins KE, Ciccarelli O, Cader MZ, Matthews PM, Behrens TE. Tract-based spatial statistics: Voxelwise analysis of multi-subject diffusion data. Neuroimage. 2006a; 31(4):1487–1505. [PubMed: 16624579]

Smith SM, Jenkinson M, Johansen-Berg H, Rueckert D, Nichols TE, Mackay CE, Watkins KE, Ciccarelli O, Cader MZ, Matthews PM, Behrens TE. Tract-based spatial statistics: Voxelwise analysis of multi-subject diffusion data. Neuroimage. 2006b

Smith SM, Johansen-Berg H, Jenkinson M, Rueckert D, Nichols TE, Miller KL, Robson MD, Jones DK, Klein JC, Bartsch AJ, Behrens TE. Acquisition and voxelwise analysis of multi-subject diffusion data with tract-based spatial statistics. Nat Protoc. 2007; 2(3):499–503. doi:nprot.2007.45 [pii] 10.1038/nprot.2007.45. [PubMed: 17406613]

Song SK, Sun SW, Ju WK, Lin SJ, Cross AH, Neufeld AH. Diffusion tensor imaging detects and differentiates axon and myelin degeneration in mouse optic nerve after retinal ischemia. Neuroimage. 2003; 20(3):1714–1722. doi:S1053811903004403 [pii]. [PubMed: 14642481]

Song SK, Yoshino J, Le TQ, Lin SJ, Sun SW, Cross AH, Armstrong RC. Demyelination increases radial diffusivity in corpus callosum of mouse brain. Neuroimage. 2005; 26(1):132–140. doi:S1053-8119(05)00022-4 [pii] 10.1016/j.neuroimage.2005.01.028. [PubMed: 15862213]

Sullivan EV, Adalsteinsson E, Hedehus M, Ju C, Moseley M, Lim KO, Pfefferbaum A. Equivalent disruption of regional white matter microstructure in ageing healthy men and women. Neuroreport. 2001; 12(1):99–104. [PubMed: 11201100]

Sullivan EV, Pfefferbaum A. Diffusion tensor imaging in normal aging and neuropsychiatric disorders. Eur J Radiol. 2003; 45(3):244–255. [PubMed: 12595109]

Ulug AM, Barker PB, van Zijl PC. Correction of motional artifacts in diffusion-weighted images using a reference phase map. Magn Reson Med. 1995; 34(3):476–480. [PubMed: 7500889]

Vernooij MW, Ikram MA, Vrooman HA, Wielopolski PA, Krestin GP, Hofman A, Niessen WJ, Van der Lugt A, Breteler MM. White matter microstructural integrity and cognitive function in a general elderly population. Arch Gen Psychiatry. 2009; 66(5):545–553. doi:66/5/545 [pii] 10.1001/archgenpsychiatry.2009.5. [PubMed: 19414714]

Wakana S, Jiang H, Nagae-Poetscher LM, van Zijl PC, Mori S. Fiber tract-based atlas of human white matter anatomy. Radiology. 2004; 230(1):77–87. [PubMed: 14645885]

Witelson SF. Hand and sex differences in the isthmus and genu of the human corpus callosum. A postmortem morphological study. Brain. 1989; 112(pt 3):799–835. [PubMed: 2731030]

Wood, P.; Bunger, RP. The biology of the oligodendrocyte. In: WT, N., editor. Oligodendroglia. New York: Plenum Press; 1984. p. 1-46.

Xu J, Kobayashi S, Yamaguchi S, Iijima K, Okada K, Yamashita K. Gender effects on age-related changes in brain structure. AJNR Am J Neuroradiol. 2000; 21(1):112–118. [PubMed: 10669234]

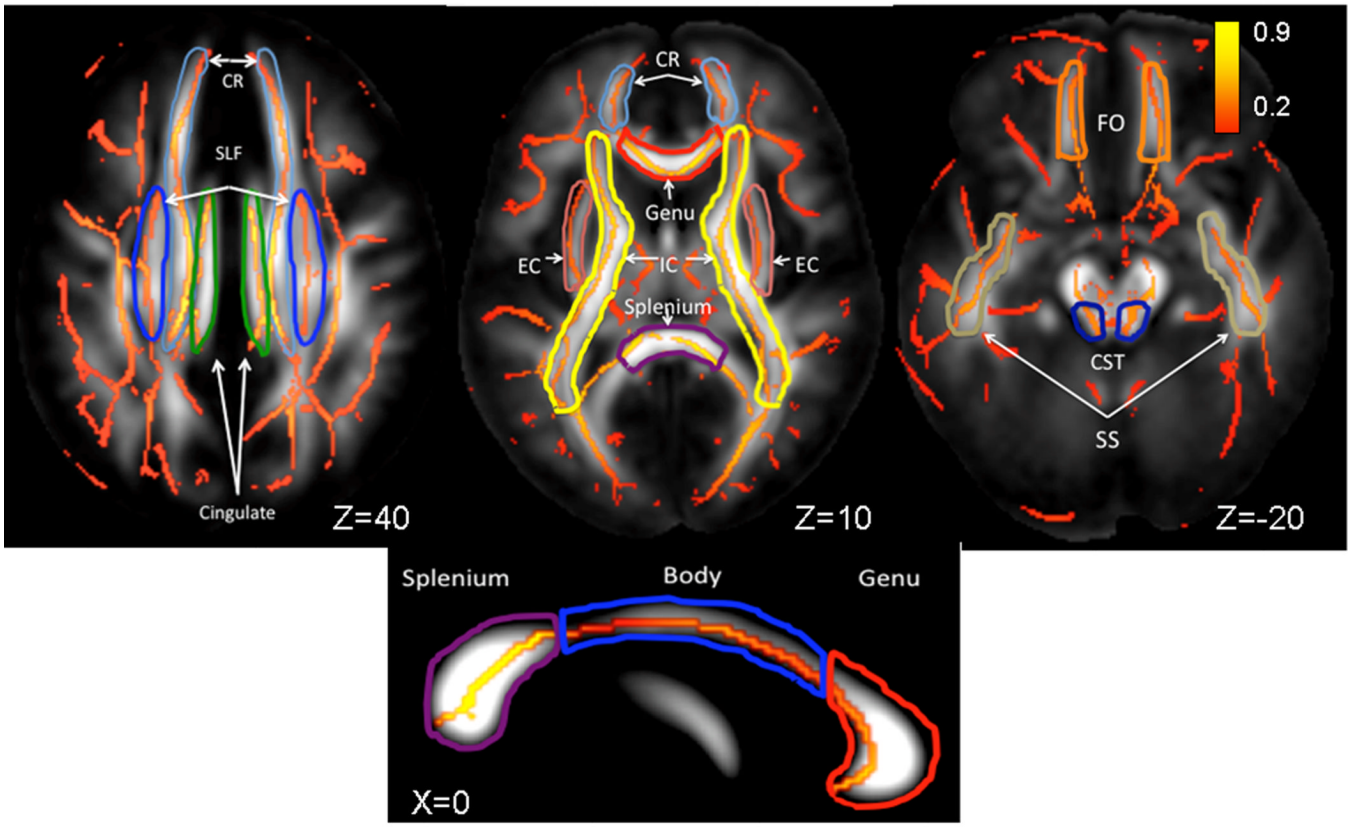

Figure 1.

Skeletonized, average FA values are shown on the population average FA image. WM-tract labels for eleven major tract are taken from John-Hopkins DTI WM atlas. The average FA values were calculated for the following tracts: CR(corona radiata), SLF (superior longitudinal fasciculus), Cingulate, EC (external capsule), IC (internal capsule), FO (fronto-occipital), CST (cortico-spinal), SS (sagittal striatum) and the Genu, Body and Splenium of Corpus Callosum

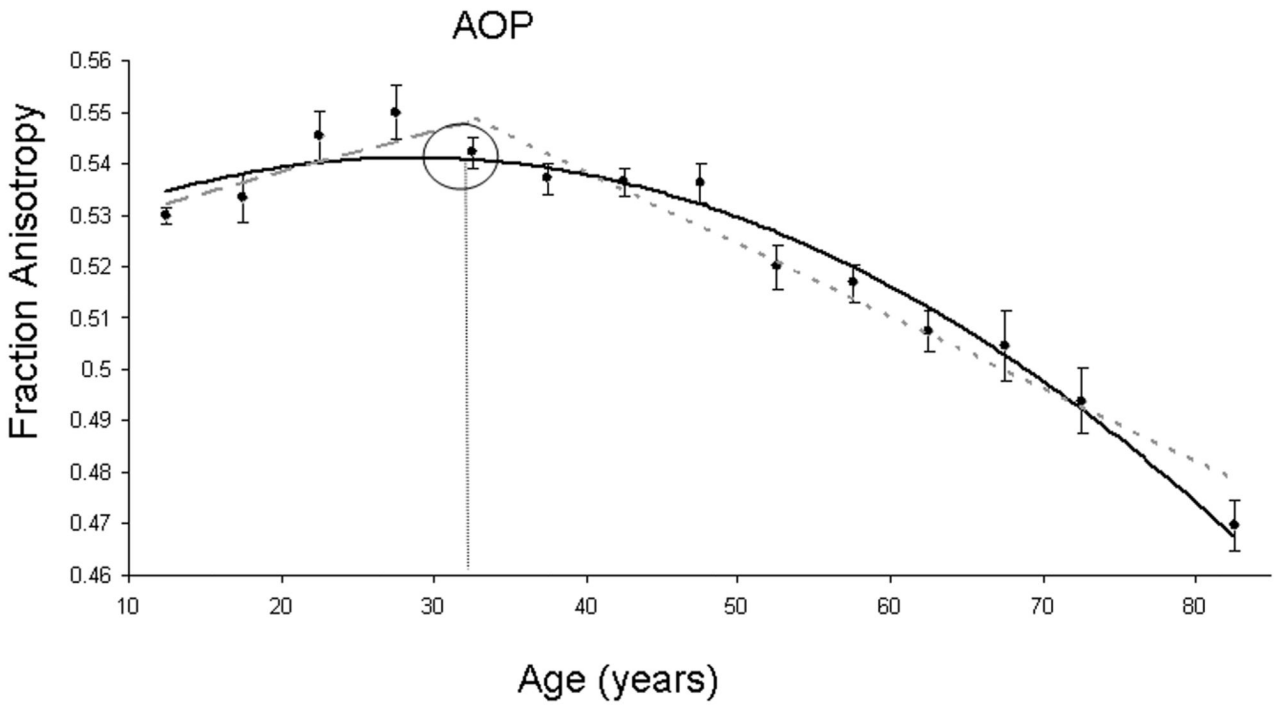

Figure 2.

Average FA values (●) stratified in 5 year intervals and age-related quadratic (solid curve, FA=0.52 + 22·10−4*age – 0.30 ·10−4*age2, r=0.49, p<1 ·10–24) and linear maturation (dashed line, FA=0.51+14.1·10−4*age, r=0.33, p=10−8) and decline (dotted line, FA=0.59–14.3·10−4*age, r=0.57, p=·10–16) trends for average FA. Age-of-peak (AOP) = 32.1±5.9 years.

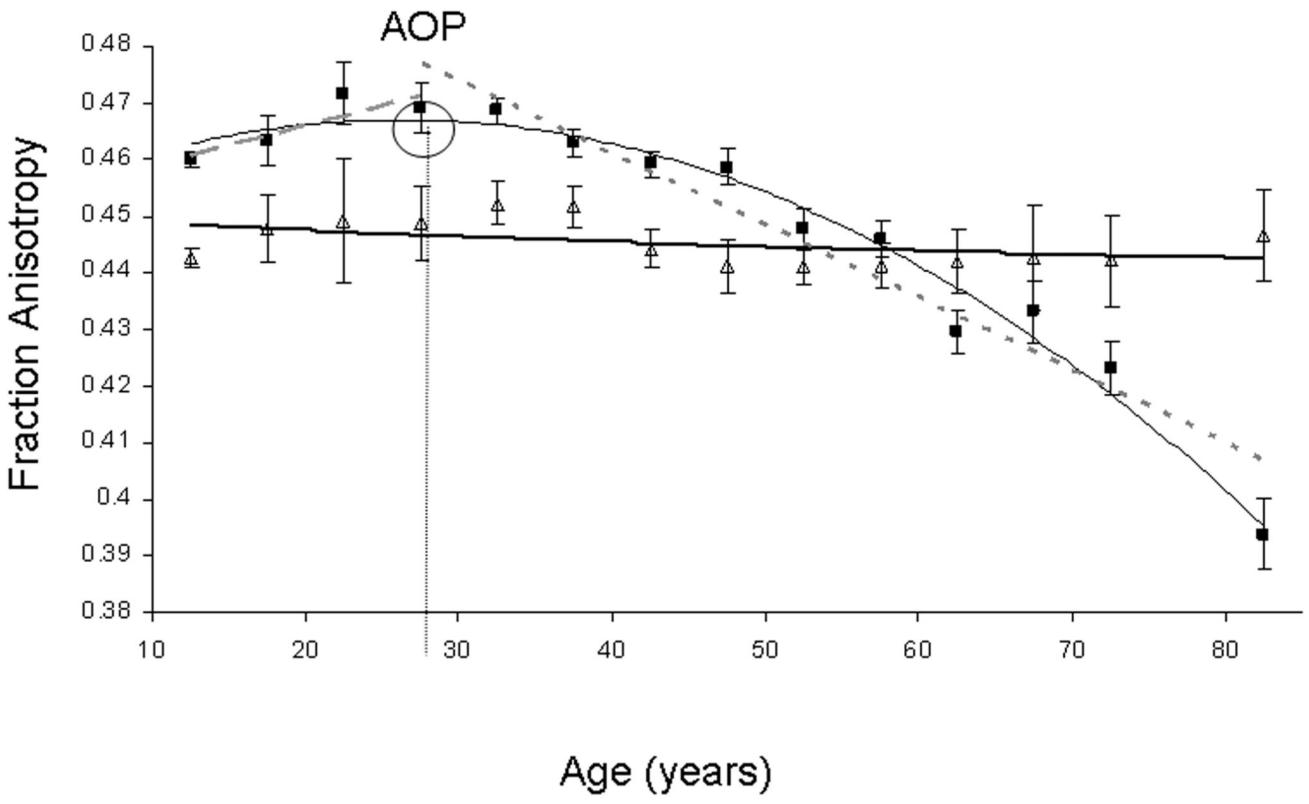

Figure 3.

FA values for Corona Radiata (■) and Cortical-Spinal tract (Δ) stratified in 5-year intervals. Age-related quadratic (thin curve, FA=0.46+15.6·10−4*age–0.27·10−4*age2, r=0.58, p<1 ·10–24) and linear maturation (dashed line, FA=0.46+4.6·10−4*age, r=0.1, p=0.8) and decline (dotted line, FA=0.51–13.3·10−4*age, r=0.64, p<10–16) trends are shown for Corona Radiata (age-of-peak (AOP)=27.9±5.7years). Quadratic (thin curve, FA=0.45+1.3·10−4*age–0.01 ·10−4*age2, r=0.17, p=0.03) trend is also shown for the Cortical-Spinal tract where the model was not significant and age-of-peak could not be calculated

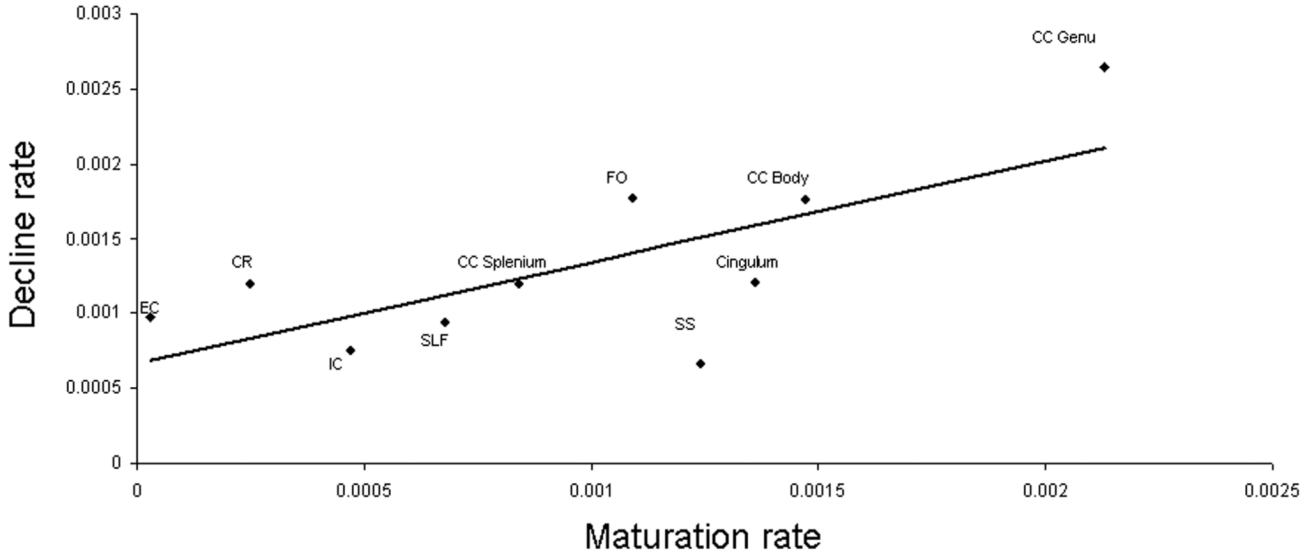

Figure 4.
By-tract FA rate of decline versus by- tract FA rate of maturation

Table 1

Subject's age distribution stratified in 5-year intervals (values ± sd)

Age Interval (years)	Average Age ± SD (years)	N subject (males/females)
11–15	13.3±0.9	254 (124/130)
15–20	15.7±1.5	25 (12/13)
20–25	22.9±1.5	20 (7/13)
25–30	27.8±1.1	34 (12/22)
30–35	33.0±1.4	88 (45/43)
35–40	38.2±1.4	59 (30/29)
40–45	43.0±1.3	72 (23/49)
45–50	48.0±1.6	50 (39/11)
50–55	53.0±1.5	52 (15/37)
55–60	58.1±1.5	54 (19/35)
60–65	62.7±1.6	48 (15/33)
65–70	67.8±1.0	24 (11/13)
70–75	73.0±1.3	24 (9/15)
75–90	80.2±4.0	27 (13/14)

Table 2

White matter tracts used in this analysis

Tract	Fiber Type	Connections
Corpus Callosum (CC), Genu, Body, Splenium	C	Cerebral Hemispheres
Cingulum	A	Cingulate Gyrus/Hippocampus
Corona Radiata (CR)	P	Cortical/Subcortical
Cortico-Spinal (CS)	P	Cortical/Spinal Cord
External Capsule (EC)	A	Frontal/Temporal/Occipital
Internal Capsule (including thalamic radiation) (IC)	P	Subcortical/Brainstem/Cortex
Superior/Inferior Fronto-Occipital Fasciculi (FO)	A	Frontal/Parietal/Occipital
Superior Longitudinal Fasciculus (SLF)	A	Frontal/Temporal/Occipital
Sagittal Striatum (SS)	A/P	Subcortical/Temporal/Occipital
C=Commissural, P=Projection, A=Association;		

Table 3

A. Results (value± sd (p-value)) of the quadratic modeling of the intersubject by-tract variability in FA values using general linear mixed effects model in eq 2.										
Tract	**Average FA**	**CC**	**Cingulum**	**CR**	**CST**	**EC**	**IC**	**FO**	**SLF**	**SS**
Average FA (A)	*.52±.02*	*.66±0.04*	*.43±.02*	*.46±.02*	*.45±.004*	*.37±0.01*	*.55±.01*	*.52±.02*	*.43±.01*	*.42±.01*
β_{age} ± sd (p)	*16.8±2.9·10^{-4} (2E-8)*	*31.9±5.5·10^{-4} (1E-8)*	*26.7±3.6·10^{-4} (3E-13)*	*13.5±2.6·10^{-4} (3E-7)*	−5.3±3.1·*10^{-4}* (.003)	*8.96±2.6·10^{-4} (0.001)*	8.9±2.4·*10^{-4}* (0.003)	*28.3±4.3·10^{-4} (1E-10)*	*10.9±2.7·10^{-4} (1E-4)*	5.4±2.6·*10^{-4}* (.04)
β_{age}^2± sd (p)	*−.26±0.03·10^{-4} (1E-13)*	*−.47±.06·10^{-4} (1E-12)*	*−.34±.04·10^{-4} (1E-14)*	*−.24±.03·10^{-4} (1E-14)*	*.064±.04·10^{-4} (3E-5)*	*−.18±.003·10^{-4} (1E-8)*	*−.14±.03·10^{-4} (1E-6)*	*−.36±.05·10^{-4} (2E-12)*	*−.19±.03·10^{-4} (1E-8)*	*−.12±.03·10^{-4} (1E-14)*
β_{sex}± sd (p)	−156.04±68.0·*10^{-4}* (.02)	−198±123·*10^{-4}* (.10)	−143±84·*10^{-4}* (.1)	−45.8±58.8·*10^{-4}* (.4)	*−191±81·10^{-4} (2E-4)*	−68.5±59.0·*10^{-4}* (0.2)	−127±56.8·*10^{-4}* (0.03)	−167±97·*10^{-4}* (.08)	−89.6±62·*10^{-4}* (0.2)	−45.8±58.8·*10^{-4}* (.4)
$\beta_{age,sex}$± sd (p)	10.8±3.9·*10^{-4}* (0.01)	13.4±7.2·*10^{-4}* (.10)	14.6±4.9·*10^{-4}* (.003)	3.2±3.4·*10^{-4}* (.3)	*17.0±4.7·10^{-4} (3E-4)*	4.0±3.4·*10^{-4}* (0.2)	7.6±3.3·*10^{-4}* (.02)	9.5±5.7·*10^{-4}* (.1)	7.0±3.6·*10^{-4}* (.05)	3.2±3.4·*10^{-4}* (0.3)
β_{age}^2,sex± sd (p)	−.14±0.1·*10^{-4}* (.001)	−.20±.09·*10^{-4}* (.10)	*−.18±.06 (0.001)*	−.06±.04·*10^{-4}* (.2)	*−.19±.05·10^{-4} (3E-4)*	−.05±.04·*10^{-4}* (0.2)	−0.09±.04·*10^{-4}* (.02)	−.1±.07·*10^{-4}* (.1)	−.08±.04·*10^{-4}* (.07)	−.02±.04·*10^{-4}* (0.6)
r/$F_{5,754}$ (p)	.49/50.5 (<1E-16)	.49/50.5 (<1E-16)	.45/40.0 (<1E-16)	.58/88.2 (<1E-16)	.17/5.5 (0.003)	.50/54.1 (<1E-16)	0.34/23.3 (<1E-16)	.37/26.7 (<1E-16)	.44/40.5 (<1E-16)	.40/30.7 (<1E-16)
Age of peak ± sd (years)	***32.1±5.9***	***33.8±6.3***	***39.4±5.8***	***27.9±5.7***	***N/A***	***25.6±7.7***	***31.7 ±9.3***	***38.9±6.6***	***28.8±7.6***	***23.1±11.6***

Table 3B. Results (value± sd (p-value)) of the modeling of the intersubject variability in FA values for three partitions of the CC using general linear mixed effects model in eq 2.			
Tract (DF=755)	**CC Genu**	**CC Body**	**CC Splenium**
Average FA (A)	.59±.05	0.62±.03	.75±.03
β_{age}± sd (p)	43.0±6.8 (1E-9)	35.1±8.0 (1E-5)	17.0±5.8 (.003)
β_{age}^2± sd (p)	−.63±.07 (1E-14)	−.55±.1 (1E-7)	−.29±.06 (1E-5)
β_{sex}± sd (p)	−43.0±152 (.8)	−43.4±178 (.9)	−501±132 (1E-4)
$\beta_{age,sex}$± sd (p)	7.4±8.9 (0.4)	7.41±10.4 (.6)	28.0±7.7 (5E-4)
β_{age}^2,sex± sd (p)	−.13±.1 (.2)	−.13±0.12 (.3)	−.34±.09 (5E-4)
r/$F_{5,755}$ (p)	.50/55 (<1E-16)	.34/22 (<1E-16)	.38/28.9 (<1E-16)
Age of peak (years)	***34.2±5.7***	***31.8±7.7***	***29.9±10.5***

Table 4

A. Results (value± sd (p-value)) of the linear modeling of the maturation and decline rates used general linear mixed effects model in eq 3.									
Tract	**Average FA**	**CC**	**Cingulum**	**CR**	**EC**	**IC**	**FO**	**SLF**	**SS**
Maturation. Average FA	*.51±0.01*	*.66±0.01*	*.40±.01*	*.46±.01*	*.38±.01*	*.55±.01*	*.49±.01*	*.43±.01*	*.40±.01*
β_{age}± sd (p)	*7.5±3.0·10^{-4} (.01)*	*10.8±5.2·10^{-4} (.05)*	*13.6±2.6·10^{-4} (1E-6)*	*2.5±4.0·10^{-4} (.5)*	*0.3±5.7·10^{-4} (.9)*	*4.7±2.9·10^{-4} (.1)*	*10.9±3.0·10^{-4} (.0001)*	*6.8±4.0·10^{-4} (.05)*	*12.4±13.0·10^{-4} (.2)*
β_{sex}± sd (p)	*−242±85·10^{-4} (.004)*	*−370±139·10^{-4} (.01)*	*−78±76·10^{-4} (.2)*	*−104±122·10^{-4} (.4)*	*−40±135·10^{-4} (.8)*	*−166±68·10^{-4} (.02)*	*−120±80·10^{-4} (.2)*	*−155±101·10^{-4} (.1)*	*31±249·10^{-4} (.9)*
$\beta_{age,sex}$± sd (p)	14.2±4.7·10^{-4} (.01)	18.4±6.7·10^{-4} (.01)	7.1±3.4·10^{-4} (.05)	6.2±8.8·10^{-4} (.4)	1.0±1.6·10^{-4} (.5)	9.1±3.9·10^{-4} (.02)	4.5±3.7·10^{-4} (.2)	10.7±6.4·10^{-4} (.1)	−3.3±18.0·10^{-4} (.9)
r/$F_{3,N}$ (p)	.33/13.0 $_{3,307}$ (1E-8)	.30/12.3 $_{3,337}$ (1E-7)	.40/29.0$_{3,403}$ (2E-16)	.01/0.8 $_{3,276}$ (0.5)	.01/0.4 $_{3,265}$ (0.7)	.22/6.7 $_{3,265}$ (.001)	.30/14.0 $_{3,395}$ (1E-9)	.17/3.5 $_{3,284}$ (.01)	.1/1.1 $_{3,254}$ (.3)
Decline. Average FA	*.58±.01*	*.78±.01*	*.50±.01*	*.51±.01*	*.42±.01*	*.59±.01*	*.60±.01*	*.48±.01*	*.45±.01*
β_{age}± sd (p)	*−11.7±1.3·10^{-4} (1E-16)*	*−21.0±2.6·10^{-4} (1E-16)*	*−12.0±1.9·10^{-4} (1E-9)*	*−12.0±1.0·10^{-4} (1E-16)*	*−9.7±0.9·10^{-4} (1E-16)*	*−6.5±1.0·10^{-4} (1E-9)*	*−14.5±2·10^{-4} (1E-9)*	*−9.4±1.1·10^{-4} (1E-16)*	*−6.7±.8·10^{-4} (1E-16)*
β_{sex}± sd (p)	*261±102·10^{-4} (.01)*	*300±218·10^{-4} (.2)*	*422±190·10^{-4} (.01)*	*87±78·10^{-4} (.2)*	*73±76·10^{-4} (.4)*	*68±87·10^{-4} (.4)*	*220±221·10^{-4} (.5)*	*97±82·10^{-4} (.2)*	*80±68·10^{-4} (.2)*
$\beta_{age,sex}$± sd (p)	−5.6±2.0·10^{-4} (.001)	−8.1±4.0·10^{-4} (.05)	−6.7±3.0·10^{-4} (.02)	−3.0±1.3·10^{-4} (.4)	−1.9±1.5·10^{-4} (.2)	−1.4±1.6·10^{-4} (.4)	−4.3±3.8·10^{-4} (.3)	−1.4±1.6·10^{-4} (.4)	−2.2±1.3·10^{-4} (.1)
r/F $_{3,N}$ (p)	.57/76.7 $_{3,408}$ (<1E-16)	.54/57.8 $_{3,373}$ (<1E-16)	.49/36.7 $_{3,304}$ (<1E-16)	.62/104.0 $_{3,459}$ (<1E-16)	.53/67.1 $_{3,479}$ (<1E-16)	.39/26.4 $_{3,408}$ (1E-16)	.41/25.1 $_{3,318}$ (<1E-14)	.50/54.6 $_{3,450}$ (<1E-16)	.45/45.2 $_{3,493}$ (<1E-16)

Table 4B. Results of the linear modeling of the maturation and decline rates for three compartment of the Corpus Callosum (CC) using general linear mixed effects model in eq 3			
Tract	**CC Genu**	**CC Body**	**CC Splenium**
Maturation. Average FA (A)	*.57±0.01*	*.61±0.01*	*.76±.02*
β_{age}± sd (p)	*21.3±5.0·10^{-4} (.001)*	*14.7±8.9·10^{-4} (.1)*	*8.4±7.1·10^{-4} (.2)*
β_{sex}± sd (p)	*−165±159·10^{-4} (.3)*	*−392±225·10^{-4} (.1)*	*−854±190·10^{-4} (1E-5)*
$\beta_{age,sex}$± sd (p)	12.3±8.2·10^{-4} (.1)	24.0±12.7·10^{-4} (.06)	47.0±12.5·10^{-4} (.001)
r/F (p)	.30/13.3 $_{3,337}$ (1E-8)	.25/6.9 $_{3,305}$ (1E-4)	.30/10.8 $_{3,286}$ (1E-6)
Decline. Average FA (A)	*.73±.02*	*.72±.02*	*.82±.02*
β_{age}± sd (p)	*−26.5±3.2·10^{-4} (1E-16)*	*−17.6±3.3·10^{-4} (1E-7)*	*−12.1±2.5·10^{-4} (1E-6)*

Table 4B. Results of the linear modeling of the maturation and decline rates for three compartment of the Corpus Callosum (CC) using general linear mixed effects model in eq 3			
Tract	**CC Genu**	**CC Body**	**CC Splenium**
β_{sex}± sd (p)	*358±266·10^{-4} (.2)*	*369±259·10^{-4} (.2)*	*408±190·10^{-4} (.03)*
$\beta_{age,sex}$± sd (p)	−8.7±4.8·*10^{-4}* (.1)	−10.7±4.9·*10^{-4}* (.03)	−9.1±3.5·*10^{-4}* (.01)
$r/F_{n,N}$ (p)	.54/56.1 $_{3,373}$ (<1E-16)	.41/32.1 $_{3,407}$ (<1E-16)	.38/29.7 $_{3,437}$ (<1E-16)